Polymer Bulletin
https://doi.org/10.1007/s00289-023-05107-7

ORIGINAL PAPER

Effect of carbon black and curing system on rubber–metal interface strength of automotive components

Michal Drobilik[1] · Martin Stenicka[1] · Marek Poschl[1] · Petr Zadrapa[1] · Radek Stocek[1]

Received: 6 September 2023 / Revised: 30 October 2023 / Accepted: 28 November 2023

Abstract

Rubber–metal parts inside the car require rubber compounds capable of ensuring optimal function and maximum service life without interface delamination. From this perspective, the strength of the bond which is created by the chemical interaction of rubber and metal by an adhesive is decisive for ensuring the functionality of the entire compound. It is dependent not only on the choice of the right adhesive but also on the rubber compound ingredients and their amount. Here, the influence of different types of carbon blacks as well as different curing systems in combination with a commonly used adhesive is described. The durability of the metal–adhesive–rubber bond is characterized by a specially designed shear strength analysis under quasi-static loading, whereas a significant influence of the structure of the carbon black has shown. It has also been observed that the presence of monosulphidic bonds has a positive effect on the shear strength.

Keywords Rubber–metal bondability · Adhesive agent · Single-lap shear test · Shear strength · Carbon black · Curing system

Introduction

Silentblocks or other metal-bonded rubber-based damping components are widely used in the automotive industry to reduce vibration and noise and provide a comfortable ride for passengers. More than 40 of these components are used. In a typical car, there are four main groups based on their location inside the car: engine, suspension, body, and exhaust systems. The design of each part must meet demanding requirements for durability, vibration damping, and resistance

✉ Martin Stenicka
stenicka@utb.cz

[1] Centre of Polymer Systems, Tomas Bata University in Zlin, tr. T. Bati 5678, Zlin 760 01, Czechia

Published online: 14 January 2024

to thermal and chemical ageing. For example, the lifetime of body system components is expected to survive approx. one million cycles. It is therefore very difficult to guarantee the optimal function of a part with such a demanding service life, and the resistance of the rubber–to–metal connection plays a key role here [1].

Today, many real products are connected mechanically (physically), e.g. by hooks, as in Fig. 1 showing a coil spring with a rubber part, or chemically by adhesive sealant. Obviously, the interface is susceptible to external influences (dust, environmental conditions, stones, etc.), coating wear, possible noise, vibration, and harshness that can affect the function of this component. These effects are eliminated by using an adhesive sealant that fills the gap between both parts and provides a protective barrier [2]. The problem is that even these components are loaded over a wide range of forces, and therefore optimal adhesion between rubber and metal is required for load transfer. For this reason, the mechanical properties of the adhesive sealant, such as tensile strength, tear strength, or elongation at break, are not sufficient to determine optimal properties.

Due to the above-mentioned problem, another adhesive with improved mechanical properties should be applied. Often, two-component (2K) structural adhesive based on acrylate is used for rubber–metal bonding with pre-activation of the rubber surface with a primer [4]. This adhesive cures chemically by radical polymerization after mixing the monomer and hardener at room temperature. The function of the primer is to wet the rubber surface and create a bridge for the bond between both materials.

Adhesive is connected to another material by adhesion, which is the attraction of two different substances due to intermolecular forces between them. This is different from cohesion, which defines the intrinsic strength of an individual material. Basically, two main failures may occur in bonding: failure between the adhesive and the rubber and cohesive failure within the adhesive. The intermolecular forces involved in both adhesion and cohesion are primarily van der Waals forces (physical adsorption) and hydrogen bonds (strong polar attraction). This type of rubber–metal bonding is shown schematically in Fig. 2 [2, 5].

Determining the shear strength by testing a real product is not always possible, and therefore standard laboratory-prepared test samples are used to simulate real conditions as much as possible.

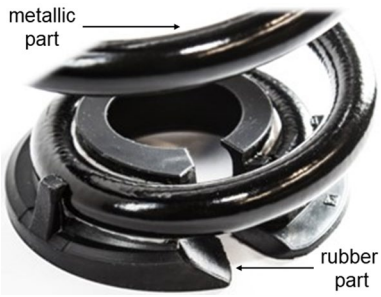

Fig. 1 Coil spring with rubber part bonded by hooks [3]

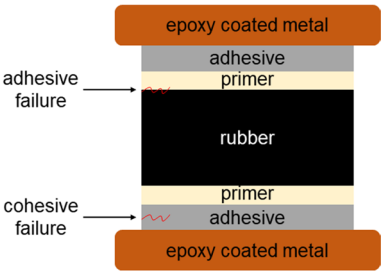

Fig. 2 Components of an adhesive joint with examples of cohesive and adhesive failure

The peel test, shown schematically in Fig. 3a, is one of the most common methods used to determine the shear strength of the interface between a rubber sample bonded to a thick metal strip. The rubber peels off the metal at a defined speed in a direction perpendicular to the bonded surface. Shear strength is then defined as the maximum fracture or separation force relative to the area of the interface [6].

Another standard method used to determine the shear strength of the bonded joint at the interface is the lap shear test, shown in Fig. 3b. This method consists of a rectangular rubber piece bounded with glue to two metal plates. Shear deformation is then achieved by applying a tensile load to the metal plates in the direction of the bond plane on the metal plate. Shear strength is defined here as the strength to failure.

Optimal adhesion between the rubber and the metal means that the required shear strength is achieved and the inside of the rubber portion tears under load acc. to DIN 53531–2 [8], indicating cohesive failure of the rubber. The optimization of the rubber recipe or the primer application process is necessary to achieve a cohesive failure in the rubber. The rubber compounds used for these automotive components are most often based on natural rubber (NR), styrene-butadiene rubber (SBR), or butadiene rubber (BR) reinforced with different types and contents of carbon blacks (CB) acc. to the given use. Often, fillers make up more than half of the total volume of the mixture; it is therefore expected that the fillers significantly affect the strength of the rubber-metal bond. Also, the complete curing system (CS) reflected in various cross-linking densities and antiageing agents such as antioxidants (AOX) and antiozonants (AOZ) can play a crucial role in achieving the optimal bonding properties and resistance to degradation processes caused by oxygen and ozone [9]. The influence of these individual factors on the strength of the connection has not yet been systematically described in the literature. Therefore, this study should be an initial insight into this problem and establish the analysis procedure to obtain the relationship between the CS composition, network density, and the type of CB on the strength of rubber–metal bonds.

Experimental part

Materials

All four rubber compounds were based on NR (SVR CV60) matrix and filled with 70 phr CB1, CB2, CB3, and CB4, respectively. CB1–CB3 (supplied by Cabot

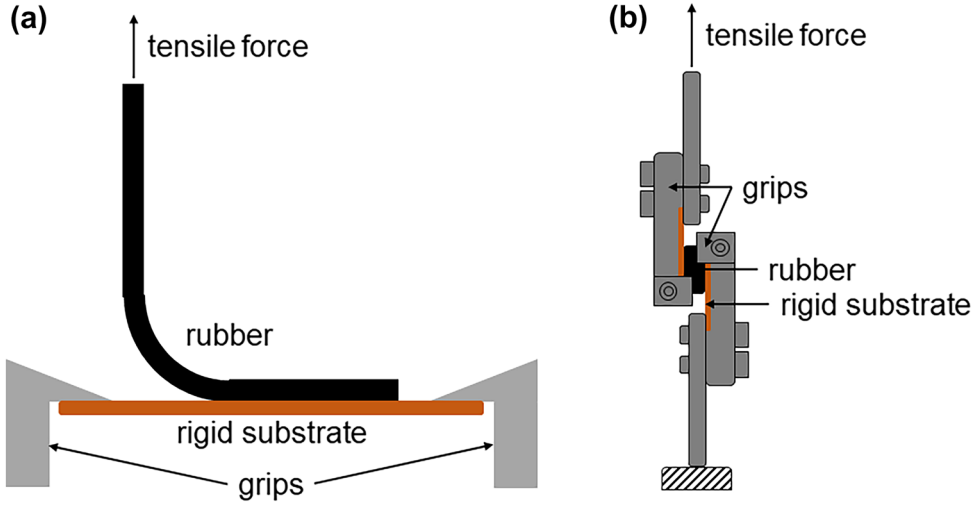

Fig. 3 Scheme of test methods used for determination of rubber–metal bonding strength: 90° peel **a** [7], single-lap shear **b**

Table 1 CB types and their basic properties [10, 11]

CB type	Nitrogen surface area (m^2/g)	OAN absorption (ml/100 g)	Production process/type
CB1	106	114	Furnace black/conventional
CB2	76	102	
CB3	39	121	
CB4	75	104	Gas black/special

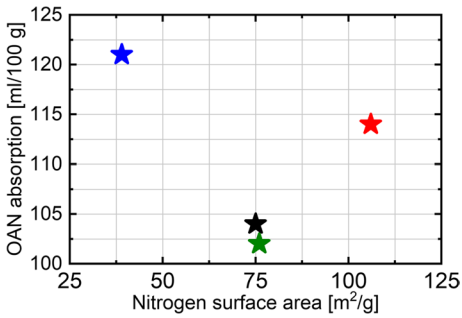

Fig. 4 Structure analysed by OAN vs. nitrogen surface area for all CB types employed. CB1 (red), CB2 (olive), CB3 (blue), and CB4 (black)

Corporation, Latvia) were produced by conventional process and differed in the diameter of particles characterized by nitrogen surface area and structure analysed by oil absorption number (OAN) acc. to ASTM D2414. CB4 (Orion Engineered Carbons, Germany) was manufactured by a special production process, which guarantees almost the same surface area and structure as CB2; however, it contains more functional groups on the surface. The basic properties of all CBs applied in the research are listed in Table 1, and mutual comparison of their particle diameters and structures is shown in Fig. 4.

Since the CB type is commonly characterized by nitrogen surface area, OAN absorption, and production process, it is assumed that a higher surface area offers more possibilities to react with the adhesive due to the functional groups (R–OH, R–COOH,…) on the CB surface [12].

It can be expressed as:

↑ Surface area: ↑ Functional groups: ↑ Rubber–metal bonding.

As the structure of CB increases (higher number of primary particles per aggregate), there should be higher amount of filler for interactions with adhesive ultimately leading to better bonding.

It can be presented like:

↑ Structure: ↑ Amount of filler: ↑ Rubber–metal bonding.

In dependence of sulphur amount, a different cross-link type is generated between rubber chains during curing process. As is well-known, the accelerated sulphur CSs are classified as conventional vulcanization (CV), efficient vulcanization (EV), and semi-efficient vulcanization (SEV) based on the amount of sulphur and the accelerators used in the respective system. Generally, the CV system is characterized by a high dosage of sulphur and a low dosage of accelerators. A

low level of sulphur and a high dosage of accelerator are used for the EV system. An intermediate level of sulphur and accelerator is employed for SEV system [13–15]. It has also been reported that the vulcanizates based on varied CSs comprise different poly-, di-, and monosulphidic cross-links. CV cured rubber has the highest amount of poly- and disulphidic cross-links, whereas EV cured rubber contains the highest amount of monosulphidic cross-links. Because of the low bond dissociation energy of the polysulphidic cross-links (252 kJ/mol) compared to the disulphidic (268 kJ/mol) and monosulphidic (285 kJ/mol) cross-links [16, 17], the network with a decreasing amount of poly- and disulphidic and increasing amount of monosulphidic cross-links should provide more free double bonds on rubber chains for a possible future bonding reaction due to the lower sulphur amount that can react with double bonds. Therefore, in the current research, different types of CS were also investigated for the strength of the rubber–metal bond.

The other ingredients and their quantities were kept the same in all rubber compounds. The complete formulations are given in Table 2. In total, 12 rubber compounds were produced.

As a glue, a commonly used 2K structural adhesive based on acrylate was selected. Before its application, propan-2-ol-based primer was used for activation of rubber surface. Glue and primer were supplied by AHES company, Czechia.

Table 2 Rubber compound recipes and CS comparison

Ingredients	CV system (phr)	SEV system (phr)	EV systems (phr)
NR (SVR CV60)	100	100	100
CB*	70	70	70
AOZ	1	1	1
AOX	1	1	1
Process oil	8	8	8
Wax	2	2	2
ZnO	5	5	5
Stearic acid	2	2	2
Sulphur	2.5	1.2	0.3
CBS	0.5	0.8	2.2
TMTD	–	0.4	1.0
Cross-link type	Estimated content of cross-links (sulphur/accelerator ratio,%)		
Monosulphidic bonds	20	50	90
Di-, polysulphidic bonds	80	50	10

*CB1, CB2, CB3, or CB4

Mixing process

The mixing process was performed in two steps. Firstly, masterbatches were prepared in an internal mixer (SYD-2L, Everplast, Taiwan) and cooled on an open mill (Farrell G-2603 150×330 mm). A similar procedure was used for the preparation of the final batches, where a CS was added to the masterbatch. The mixing process conditions are listed in Table 3.

The final batches were stored for 48 h at room temperature (RT) before curing.

Compounds rheological properties and sample production

Rheological properties, especially optimal curing time t_{90} and scorch time ts_1, for all rubber compounds were determined using moving die rheometer (MDR 3000 Basic, MonTech, Germany) at 160 °C acc. to ASTM D 6204.

Subsequently, rubber sheets of 150 mm × 150 mm in 2 mm and 6 mm thicknesses for $t_{90}+1$ min/1 mm of thickness were produced in a compression mould using a hydraulic press (LabEcon Series 300, the Netherlands) at 160 °C. Then, samples were punched out from the sheets acc. to the corresponding standards mentioned in the fundamental analyses chapter.

Apparent cross-link density

Since various CSs were employed and all rubber compounds were filled with CB, apparent cross-link density was calculated for the evaluation in the forthcoming analyses. The protocol to apparent cross-link density calculation was based on the Kraus modified Flory–Rehner equation for filled rubber vulcanizates from equilibrium swelling in toluene [18, 19]; its complete version can be found in Ref. [18].

For the swelling test, three rectangular samples for each rubber compound were punched out in dimensions of 20×30×2 mm. After initial weighting, the samples

Table 3 Mixing process

First step: masterbatch			
Ingredients	Machine	Temperature (°C)	Dosing/ total time (min)
NR (SVR CV60)	Internal mixer	60 → 130	0/7
2/3 CB			2/7
1/3 CB + Process oil			4/7
Stearic acid, ZnO, AOX, AOZ, Wax			5/7
	Open mill (cooling, shaping)	60	0/3
Second step: final batch			
Masterbatch, CBS, TMTD, sulphur	Internal mixer	60 → 100	0/3
	Open mill (cooling, shaping)	60	0/3

were immersed into a flask containing toluene and left to swell. The samples were regularly weighed up until their weight equilibrium, which was reached after 10 days. Then, the average value of apparent cross-link density was calculated. The whole experiment was performed at RT.

Fundamental analyses

Fundamental analyses were performed for all rubber compounds. Hardness Shore A was measured acc. to ISO 7619–1 on hardness meter (Polymertest, Czechia) for five measurements of each compound. Rebound resilience was measured acc. to ISO 4662 on an instrument for determining rebound elasticity Schob (Polymertest, Czechia) three times on two samples for each compound. The tensile properties like tensile strength and elongation at break were determined acc. to ISO 37 on tensile test machine Testometric M350-5CT (Testometric, the UK) for four samples of each compound, using dumb-bell samples, type S2. The tear test was performed acc. to ISO 34–1 on the same tensile testing machine for three samples of each compound using trouser samples.

Single-lap shear sample preparation and testing

Single-lap shear samples consisting of a rubber part and metal were prepared in several steps. Firstly, a punched rubber sample with dimensions 25 mm × 25 mm × 6 mm and epoxy-coated metal plate surface were cleaned by cleaner based on petrol fraction and rested for 10 min. Then, a thin layer of primer (approx. 0.1 mm) was applied on one side of rubber and rested for 10 min. Afterwards, adhesive was applied on the rubber surface, and both parts, rubber and metal, were compressed to the final glue layer thickness 0.5 mm. The same procedure was performed on the other side of the rubber part. The complete procedure is shown in Fig. 5.

The prepared single-lap shear samples were stored for 72 h at RT to achieve optimal curing of adhesive. Then, the test was performed acc. to DIN 53531–2 on servo-hydraulic tensile machine Instron 8871 (Instron, the UK) for four samples of each compound with the tensile rate of 15 mm/min. The special clamping system for test samples is shown in Fig. 3b.

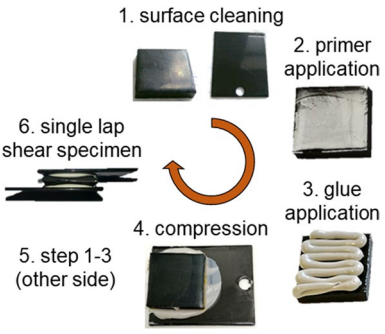

Fig. 5 Single-lap shear sample preparation

The shear strength was calculated as the ratio of the measured shear force to sample cross-section (25 mm^2) acc. to Eq. (1):

$$\text{Shear strength [MPa]} = \frac{\text{Shear force [N]}}{\text{Sample cross-section } [\text{mm}^2]} \quad (1)$$

Results and discussion

Rheological properties

Rheological curves are plotted in Fig. 6a–c. The scorch time ts_1 (Fig. 7a) was determined in a relatively narrow range (1.3–2.3 min), whereas curing time t_{90} (Fig. 7b) oscillated from 2.6 to 7.8 min. The expectation that ts_1 and t_{90} for different CS will decrease as follows: CV < SEV < EV was not observed. The possible explanation can be found in the content of individual CS, where a combination of two different types of accelerators was employed. And, since TMTD is significantly faster accelerator than CBS, as was confirmed by Movahed et al. [20], their concentrations have to be taken into account. In the employed CS, the mutual ratio TMTD/CBS was 0:0.5, 1:2, and 1:2.2 for CV, SEV, and EV, respectively. This order (CV < EV < SEV) already correlates with the obtained times very well and the efficiency of individual

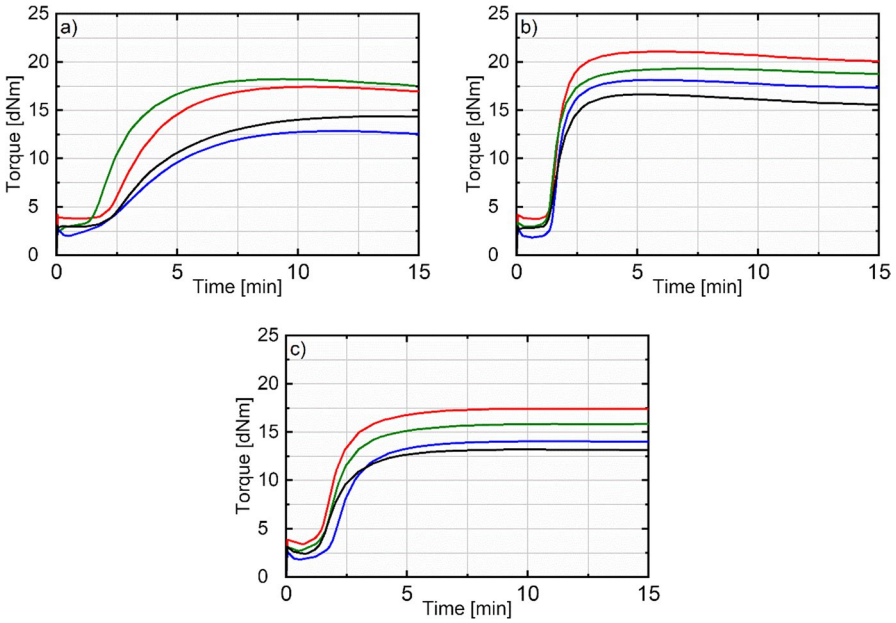

Fig. 6 Torque vs. time for all rubber compounds: CB1 (red), CB2 (olive), CB3 (blue), and CB4 (black) and all curing systems: CV **a**, SEV **b**, and EV **c**

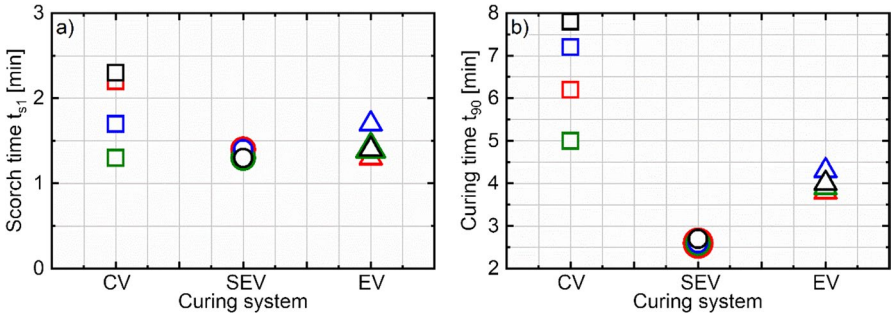

Fig. 7 Scorch time t_{s1} **a** and curing time t_{90} **b** vs. curing system for all rubber compounds: CB1 (red), CB2 (olive), CB3 (blue), and CB4 (black)

accelerators seems to be a controlling parameter rather than sulphur/accelerator ratio.

Apparent cross-link density

Apparent cross-link density of all rubber compounds is presented in Fig. 8. As can be seen, it is in the range of 69–168 µmol/cm^3 for CV, 175–247 µmol/cm^3 for SEV, and 117–284 µmol/cm^3 for EV.

The expectation that CB type will influence the apparent cross-link density was not observed. The values decrease for each CS as follows: CB3 > CB2 > CB1 > CB4 unlike those of CV, where the lowest value was determined for CB1.

The main effect is in the content of individual CS, where the combination of two different accelerators and sulphur amount plays a significant role. This trend was observed by Movahed et al. [20], where the apparent cross-link density decreased with the increasing amount of CBS and decreasing amount of sulphur.

Basic mechanical properties

The results of basic mechanical properties are presented in Fig. 9a–f.

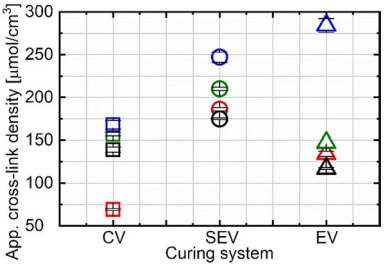

Fig. 8 Apparent cross-link density vs. curing system for all rubber compounds. Symbols denoted as in Fig. 7

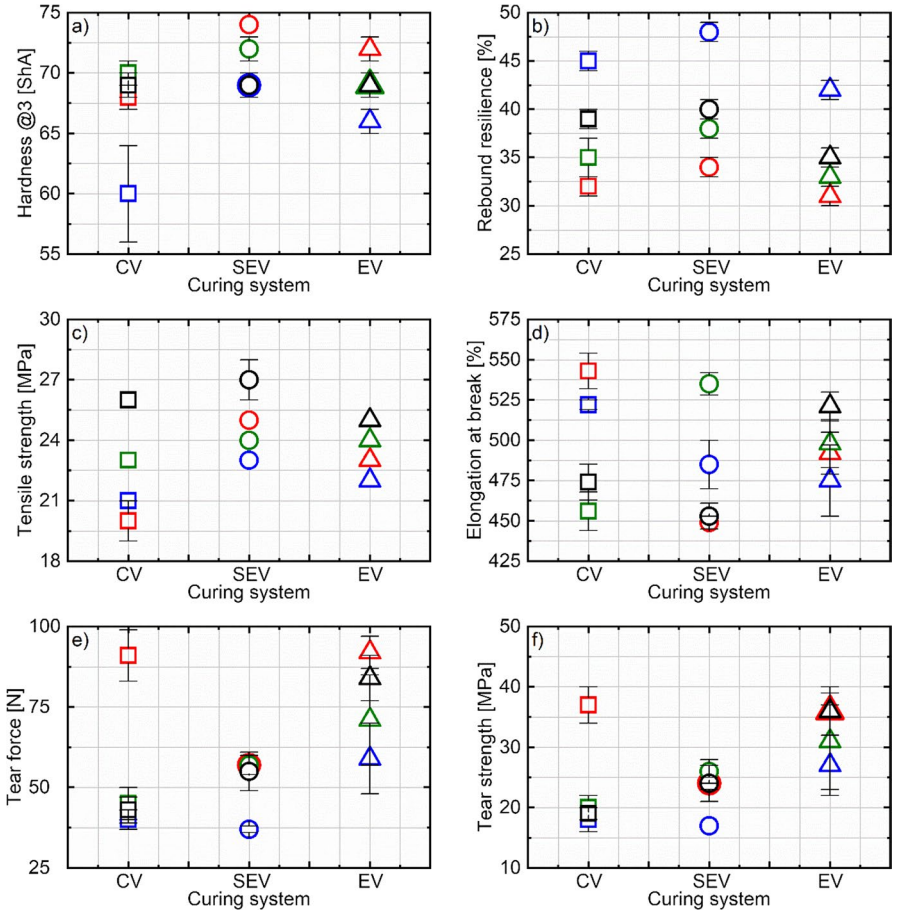

Fig. 9 Hardness **a**, rebound resilience **b**, tensile strength **c**, elongation at break **d**, tear force **e**, and tear strength **f** vs. curing system for all rubber compounds: symbols denoted as in Fig. 7

The determined hardness for all samples is in the range of 59.9–73.7 ShA. As can be seen, the results correlate with general theory; the more reinforcing CB type means higher the hardness (e.g. CB1 vs. CB3).

As Fig. 9 reveals, the samples containing CB3 show the highest rebound resilience compared to others. The values decrease for each CS as follows: CB3 > CB4 > CB2 > CB1.

The tensile properties like the tensile strength and the elongation at break are in the range of 20.4–27.0 MPa, respectively, 453–535% for all samples. The highest tensile strength has CB4–SEV and conversely the lowest CB1–CV.

The tear force demonstrates the needed energy to rip the prepared sample and cause crack to continue until it breaks. As shown in Fig. 9, the samples with CB1 display the highest tear force and conversely the samples with CB3 the lowest one.

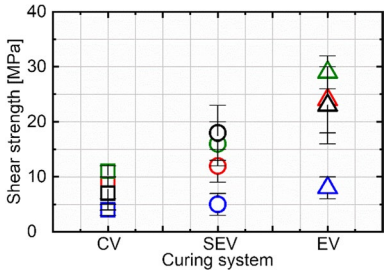

Fig. 10 Shear strength vs. curing system for all rubber compounds. Symbols denoted as in Fig. 7

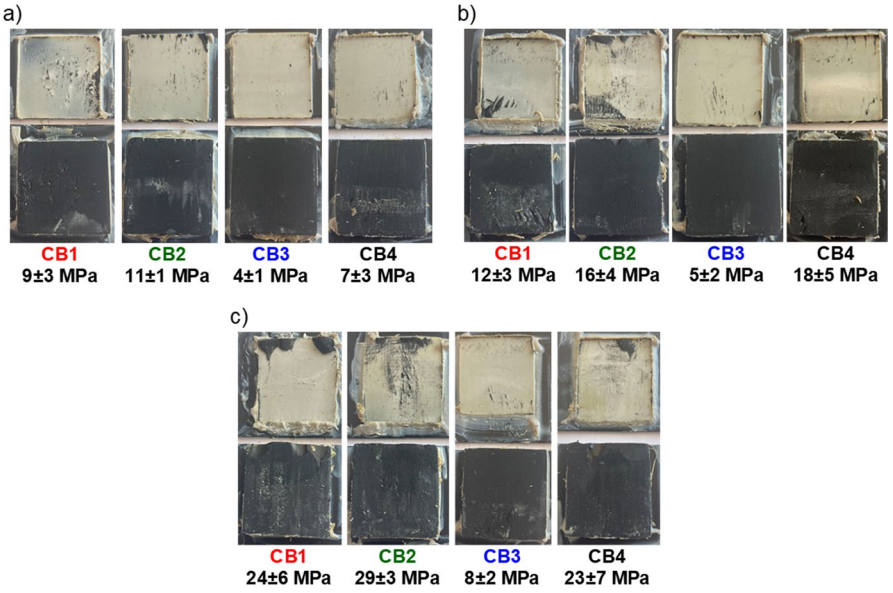

Fig. 11 Snapshots of representative specimens for each rubber compound after single-lap shear test. Shear strength values and their standard deviations for each rubber compound are included for various curing systems: CV **a**, SEV **b**, and EV **c**

Shear strength

The results from the single-lap shear test in Fig. 10 show that the lowest shear strength, 4.0 MPa, was determined for CB3–CV, whereas the highest shear strength, 29.0 MPa, for CB2–EV. In Fig. 11, the snapshots of representative specimen after the single-lap shear test are shown.

The effect of CB structure reflects in the shear strength; the highest was found for CB2 and CB4 (with the lowest structure), whereas the lowest shear strength was measured for CB3, which has the highest structure.

A significant role was played by the choice of CS for the compound. Here, it can be stated with only very few exceptions (CB3–EV, CB3–SEV) that the EV systems provided the highest values, and on the contrary, CV system showed the lowest

ones. This seems to be strongly connected with the cross-link type, where a higher content of monosulphidic bonds has a more positive effect on bondability than the apparent cross-link density due to the lower sulphur amount in EV system for curing process. This difference is clearly demonstrated here, e.g. between CB2–CV and CB2–EV: they have a similar apparent cross-link density, but CB2–EV has nearly three times higher shear strength.

Simultaneously, the own hypothesis that CB4 with oxidized surface helps to achieve higher shear strength than standard CB types was not confirmed.

The results from supporting analyses give us an overview of the range of values for each property in which the compound should be to achieve optimal bonding performance. These ranges, summarized in Table 4, can serve as a guide for the design of bondable compound.

The joint effect of CB and CS on the shear strength can be observed. The medium reinforcing CB2 type and EV system are the best choices to achieve optimal bonding between rubber and metal. Thus, a functional element produced from the sample CB2–EV would have the best bonding performance, durability, and service lifetime out of all investigated samples.

Conclusion

Experimental research focused on the effect of CB type and CS on the bonding performance between rubber and metal parts for automotive applications has been investigated. The results of shear strength and observed interrelations between CB and CS have been taken into account in the design of rubber–metal-bonded functional element to ensure optimal function and durability. A single-lap shear test revealed the shear strength for compounds filled with different CB types cured by various CSs. This enabled finding the right direction for rubber compound design.

This research shows the manner how to enhance the durability of rubber–metal-bonded products for automotive applications. It means fewer failures of products, lower development costs, and optimal functional properties for comfortable driving.

Table 4 Optimized rubber recipe and required properties

Ingredients	Type
CB	CB2
CS	EV
Properties	Required values
Apparent cross-link density	100–150 μmol/cm^3
Shore hardness	68 –72 ShA
Rebound resilience	30–40%
Tensile strength	23–26 MPa
Elongation at break	500–550%
Tear strength	15–35 MPa

Nevertheless, to better understand the effect of CB and CS on bonding performance, the deeper analysis of rubber surface by Fourier transform infrared spectroscopy, contact angle measurement, and other methods must be investigated in ongoing research. However, even at this stage the achieved results and knowledge can help to design new rubber compounds for rubber–metal applications acc. to the requirements on the final product.

Acknowledgements Authors would like to express many thanks to Mr. Hauke Westenberg from Orion Engineered Carbons company for providing CB4 for this work.

Funding Open access publishing supported by the National Technical Library in Prague. This study was funded by Ministry of Education, Youth and Sports, DKRVO (RP/CPS/2022/006).

Data availability Data will be made available on request.

Declarations

Conflict of interest The authors declare that they have no known competing financial interests or personal relationships that could have appeared to influence the work reported in this paper.

References

1. Asano E, Taguchi T, Sugiura T et al (2014) Small and lightweight anti-vibration rubber products. Sei Tech Rev 79:47–50
2. Petrie EM (2000) Handbook of adhesives and sealants. McGraw-Hill, New York
3. Wittek MA, Gaska D, Lazarz B et al (2016) Coil springs in passenger cars – general theoretical principles and structural requirements. Arch Automot Eng 72:141–159. https://doi.org/10.14669/AM.VOL72.ART9
4. Goss B (2010) Practical guide to adhesive bonding of small engineering plastic and rubber parts. Smithers Rapra Technology, Akron, pp 61–73
5. Banduhn N, Brede B, Gierenz G et al (2004) Educational materials. Bonding adhesive textbook. Springer, New York, pp 14–30
6. Brown R (2006) Physical testing of rubber. Springer, Cham, pp 363–368
7. Awalekar YJ, Takalkar AS, Shinde SS (2018) Investigation of peel resistance of adhesives materials: a review. Proc Eng Technol Innov 10:19–28
8. DIN 53531–2 (1990) Determination of the adhesion of rubber to rigid materials using conical ended cylinders
9. Liu XA, Shangguan WB (2014) Elastomeric components for noise and vibration isolation and control in the automotive industry. Enc Automot Eng. https://doi.org/10.1002/9781118354179.auto160
10. Rodgers B (2004) Rubber compounding chemistry and applications. CRC Press, Boca Raton, pp 247–282
11. Orion Engineered Carbons (2018) CK3 product datasheet
12. Kang MJ, Heo YJ, Jin FL et al (2016) A review: role of interfacial adhesion between carbon blacks and elastomeric materials. Carbon Lett 18(1):1–10. https://doi.org/10.5714/CL.2016.18.001

13. Akiba M, Hashim AS (1997) Vulcanization and crosslinking in elastomers. Prog Polym Sci 22(3):475–521. https://doi.org/10.1016/S0079-6700(96)00015-9
14. Kruzelak J, Sykora R, Hudec I (2016) Sulphur and peroxide vulcanisation of rubber compounds – overview. Chem Pap 70(12):1533–1555. https://doi.org/10.1515/chempap-2016-0093
15. Dijkhuis KAJ, Noordermeer JWM, Dierkes WK (2009) The relationship between crosslink system, network structure and material properties of carbon black reinforced EPDM. Eur Polym J 45(11):3302–3312. https://doi.org/10.1016/j.eurpolymj.2009.06.029
16. Sathi GS, Harea E, Machu A et al (2021) Facilitating high-temperature curing of natural rubber with a conventional accelerated-sulfur system using a synergistic combination of bismaleimides. Express Polym Lett 15(1):16–27. https://doi.org/10.3144/expresspolymlett.2020.68
17. Sathi GS, Stocek R, Kratina O (2020) Reversion free high-temperature vulcanization of cis-polybutadiene rubber with the accelerated sulfur system. Express Polym Lett 14(9):823–837. https://doi.org/10.3144/expresspolymlett.2020.68
18. Poschl M, Stocek R, Zadrapa P (2023) The effect of apparent cross-link density on cut and chip wear in natural rubber. Degrad Elastom Pract Exp Model 289:273–291. https://doi.org/10.1007/12_2022_129
19. Kim DY, Park JW, Lee DY et al (2020) Correlation between the crosslink characteristics and mechanical properties of natural rubber compound via accelerators and reinforcement. Polymers 12(9):1–12. https://doi.org/10.3390/polym12092020
20. Movahed SO, Ansarifar A, Mirzaie F (2015) Effect of various efficient vulcanization cure systems on the compression set of a nitrile rubber filled with different fillers. J Appl Polym Sci 132(8):1–10. https://doi.org/10.1002/APP.41512